

Medical image Synthesis with improved Deep Convolutional Bi-Generative Adversarial Network Aided Genetic Algorithm

Neeraj Varshney, Narendra Mohan
Department of Computer Engineering & Applications
GLA, University, Mathura, India-281406
neeraj.varshney@gla.ac.in ,narendra.mohan@gla.ac.in,

Article Info

Volume 82

Page Number: 56 - 63

Publication Issue:

January-February 2020

Abstract

In different clinical applications, important role is played by Medical imaging. Acquisition of various image models are limited by radiation dose and cost considerations. Desired image modality are estimated by medical image synthesis without original scan. To address this issues, generative adversarial method is proposed in this research. For a given source image, target image is generated by training fully convolutional network (FCN). Better model of FCN is obtained by using adversarial learning method. Mapping of source to target imaging is done in an effective way by this and highly accurate target images are produced by this. Generation of target images with blurring is avoided by incorporating loss function with image-gradient-difference in the design of FCN. Network is trained using Long-term residual unit. Deep convolutional adversarial network with context awareness is created by applying Auto-Context Model (ACM).

Deep Convolutional GA connected with bi-generative adversarial network (DC-Bi-GAN) is implemented for synthesizing images. From source images, target images are accurately synthesized by proposed model and it is more robust as shown by results of experimentation. From MRI, CT is generated and from 3T MRI, 7T MRI are generated using this model with three datasets. In all task and dataset, superior results are produced by proposed model.

Article History

Article Received: 14 March 2019

Revised: 27 May 2019

Accepted: 16 October 2019

Publication: 01 January 2020

Keywords: Generative Adversarial Network, Residual Learning, Image Synthesis, Deep Learning, Auto-Context Model, Adversarial Learning

1 Introduction

In planning radiotherapy, Computed tomography (CT)-based radiotherapy is used widely and it is an effective method. Compared with CT scan, superior contrasts of soft tissue are given by magnetic resonance (MR) imaging. So, developed a MR imaging based radiotherapy devices. In organs, ligaments, soft tissues, very slight differences are detected using MR imaging in an effective way. But MRI is too costly and requires more time. For example, CT requires only 5 min, while 30 min is required by MRI. MR imaging procedure is contraindicated due to artificial joints, cardiac pacemakers. Due to high cost, few patients are not adapting this.

It requires certain modality and in practice, it is not feasible, as mentioned above. From various sources, image can be synthesized by a system. It is done by acquisition protocols and image modalities. For clinical

usage, imaging data can be provided by this. It does not require any additional cost or real acquisition. It difficult to solve directly medical image synthesis. Mapping of source and target images is highly dimensional one. MRI and CT images are having various appearances as shown by figure 1 a and 1 b.

Mapping of MRI and CT image is a non-linear task. Model has to put lot effort in bridging significant gap in appearance. Compared with 3T MRI, high contrast and resolution is contained by 7T MRI as shown in figure 1 c. So mapping of 7T MRI from 3T MRI is a challenging task. To address this issue, various models are developed in recent days by various researchers. Berker et al. [1] formed various classes of tissues by segmenting MRI images in order to make MRI-to-CT problem as a task of segmentation. Known attenuation property is assigned to every class.

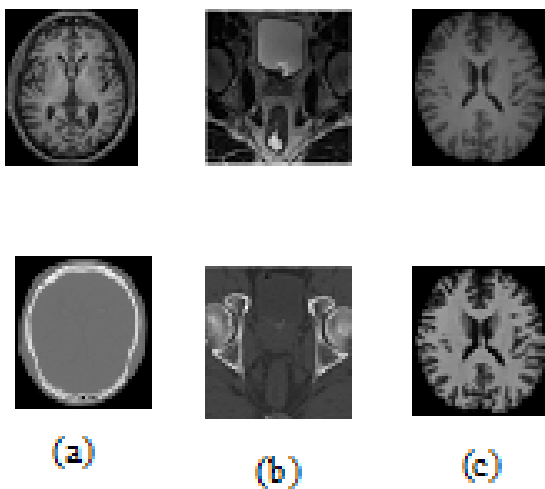


Fig. 1. Three pairs of corresponding source (left) and target (right) images from the same subjects. (a) shows a pair of MRI/CT brain images; (b) shows a pair of MRI/CT pelvic images; (c) shows a pair of 3T/7T brain MRI.

Accuracy of segmentation defines this method. Accuracy of result requires manual computation. In literature, atlas-based methods are used. New subject's source image is register an atlas in [2] and target image is estimated by wrapping atlas of corresponding target image. Label Propagation (LP) segmentation algorithm is extended in [3]. It is called as Modality Propagation.

LP generalization is allowed by this and it works with continuous data. It does not require labels categorical segmentation. Information propagation method is proposed in [4]. In source dataset, similar patches of specified source path is searched by system. According target, target images are constructed.

Accuracy of registration defines the accuracy of atlas-based methods. Mapping of source to target image can also be done with learning-based methods. It rectifies various drawbacks previous works [5]. , Jog et al. [6] performed cross-modality synthesis by nonlinear regression in high resolution images with random forest from low resolution scans.

Huynh et al. [7] used random forest to map MRI to CT. They used unsupervised methods also. Zhao et al. [8] synthesized CT from MR image using a modified U-Net [9]. Segmentation of brain is done using this synthetic MR image. In output blurs are generated by minimization of voxel-wise loss in training between reference and synthesized image.

Nie et al. [10] produced clear results by combining adversarial loss and voxel-wise loss of generative adversarial network (GAN). Positron emission tomography (PET) images are synthesized using a similar method from CT images [11]. Isola et al. proposed pixel-to-pixel (pix2pix) framework by using various information from different channels [12].

Ben-Cohen et al. [13] exported initial results by combining pix2pix model and fully convolutional network (FCN) [14]. From CT image, synthesized PET image is generated by blending two outputs. Blurry generated synthesis problem is addressed by combining adversarial loss and of voxel-wise loss. Large number of MR and Ct images which are aligned defined voxel wise lose.

It is expensive as well as difficult to get aligned data. Generated a set of target candidate values for every voxel in source image in a framework proposed in [15]. In target image's training set , nearest neighbours are searched for the same. Paired data is not used. Similarity measures are used to face the changes in modality. Mutual information is also used in this conditions. Global energy function is maximized for selecting best candidates. Between target and source, mutual information is also considered.

Source images are represented by features and target images are generated by mapping those feature. Representation of source image and manually engineered features defines performance this method. In medical image analysis and computer vision, deep learning is getting popular. It does not require any hand-crafted features for producing better results [16]. Dong et al. [17] used Convolutional Neural Networks (CNNs) for single image super-resolution. Kim et al. [18] proposed recursive CNN for improving super-resolution algorithm. Parametric complexity is not increased while boosting performance.

Li et al. [16] estimated missing PET by applying deep learning model from MRI data. Huang et al. [20] conducted synthesis of cross-modality and super-resolution medical image simultaneously. It is done by joint convolutional sparse coding which is weakly supervised. In the prediction of target image, neighbourhood information are neglected in CNN. For image synthesis, structural information is preserved by Fully Convolutional Networks (FCNs) [21]. FCN and CNN are trained using a loss function computed by L2 distance which is predicted between original and target image. In multi-modal distributions, target images are

blurred [22]. Peak signal-to-noise rate (PSNR) is maximized by reducing L2 loss. But better results are not produced by high PSNR [23].

To address this issues, generative adversarial method is proposed in this research. For a given source image, target image is generated by training fully convolutional network (FCN).

Better model of FCN is obtained by using adversarial learning method. Mapping of source to target imaging is done in an effective way by this and highly accurate target images are produced by this. Generation of target images with blurring is avoided by incorporating loss function with image-gradient-difference in the design of FCN. Network is trained using Long-term residual unit. Deep convolutional adversarial network with context awareness is created by applying Auto-Context Model (ACM).

Deep Convolutional GA connected with bi-generative adversarial network (DC-Bi-GAN) is implemented for synthesizing images. From source images, target images are accurately synthesized by proposed model and it is more robust as shown by results of experimentation. From MRI, CT is generated and from 3T MRI, 7T MRI are generated using this model with three datasets. In all task and dataset, superior results are produced by proposed model.

2 Proposed Methodology

A deep convolutional adversarial network framework is proposed to address the above mentioned challenges. In this generator corresponds to FCN and discriminator corresponds to CNN. From source images, target images are estimated by 3DFCN. 3D spatial mapping is enhanced by adapting 3D model. Across 2D slices, problems of discontinuity are solved by this. Network is designed by using adversarial learning technique. Extra discriminator network is modelled. This makes the generator output equals the target image.

In this los function is incorporated with image gradient difference. This is done to maintain generated target image's sharpness. Network is trained using the long-term residual unit. Generator output is refined iteratively by using ACM. Overlapping patches are formed by splitting input source image in testing phase. Generator estimates the target for every patch. Source-to-target synthesis is completed by merging all target patches that are generated into a single image. Overlapping CT region's intensities are averaged to perform this.

Source-to-target image synthesis used in Bi-GAN framework is described in following section. Figure 1

shows the proposed method's overall structure. It has Bi-GAN with GA. From a large set covering large area, parameters are optimized by using Bi-GAN. From a small set of choices, discrete decisions are made by using GA. Activation functions are included in choice making. Usage of batch normalization, max pooling and dropout are decided. Number of dense and convolutional layers and convolutional layer kernel size are computed.

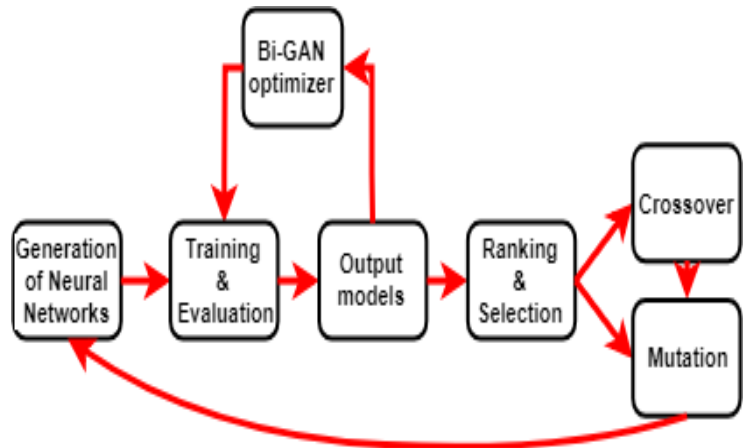


Fig. 1: Proposed Bi-GAN aided GA network for refining deep neural network parameters. For GA, network i 's parameter set is given by,

$$p_i^{GA} = \left[pr_i^{con v^1}, \dots, pr_i^{con v^C}, pr_i^{dens e^1}, \dots, pr_i^{dens e^D} \right],$$

$$i \in \{1, 2, \dots, n_m\}$$

Where, parameter is represented by pr, convolution layer is represented by conv and dense layer is represented by dense, maximum number of possible convolution layers is given by C and maximum number of possible dense layers is given by D, number of network models in population is represented as n_m .

Bi-GAN network: Generative adversarial network (GAN) which is a modified as well as novel network is proposed. It termed as Bi-GAN. From large range of values, optimum network parameters are computed. Figure 2 shows the proposed Bi-GAN network. Various neural network parameters are refined by this network. There are discriminator, evaluation part and generative part. It has one discriminator (D), two evaluators (E_1 and E_2) and are two generators (G_1 and G_2). Gaussian noise $z \sim p_{noise}(z)$ is given as input to two generators. Training data $x \sim p_{data}(x)$ is given as input to evaluators.

several big kernels to decrease the depth of the network in the generator. Our kernel size setting is empirical, and we believe that other possible configurations can also be used. There are 9 layers in this including ReLU operations, batch normalization (BN) and convolution.

One convolutional layer is included in last layer. Estimate of target image corresponds to the output of it. Pooling is not used. Feature map's spatial resolution is reduced by pooling. Effective receptive fields are not guaranteed by generator's traditional convolution operation as shown in figure 2. So, in order to obtain enough receptive field, dilated convolution is adapted. In Figure 2, 1 and 2 are the generator's first and last convolutional layer's dilation.

Typical architecture of CNN corresponds to discriminator D. It has three convolutional stages. They are max pooling, ReLU, BN. It also has three fully connected layers and one convolutional layer. ReLU activation function is used in first two fully connected layers and sigmoid function is used by third layer. Size of the filter is $3 \times 3 \times 3$. Filter number of convolutional layer corresponds to 256, 128, 64, 32 and fully connected layer has 1, 128 and 512 nodes.

Auto-Context Model (ACM) for Refinement:

Inside patch, context information available to train every training sample is limited because it is patch based. Network's modelling capacity is affected by this. ACM is used for enlarging the context in training stage. Semantic segmentation uses this commonly. Iteratively, various classifiers are trained. Previous classifier's output probability map and original image features are used to train the classifiers. Additional information of context is given by previous classifier output. This can be used by subsequent classifiers. For every classifier, input are processed one by one during test time. Initial input are concatenated with probability. Regression tasks based on deep learning can also be applied with ACM. Generated results are refined iteratively by adapting ACM. By this way, GAN is made aware about context.

Various GANs are trained iteratively. Form source and target patches inputs are taken. Second channel is concatenated with these patches with source patch. Next GAN are trained using both of this inputs. Figure 5 shows the illustration of this scheme. ACM uses same architectures of GANs. It is shown in figure 2.

Generator input are different between these two architectures. Synthetic target patch and source MRI patch are concatenated by this. In refinement based on

ACM, same size of input patch is maintained. From entirely estimated previous target image, extract the context information. Information which are not in initial input image patch are encoded.

3 Experiments and Results

In two tasks, proposed model is tested using three datasets. From corresponding MRI data, CT images are estimated from brain and pelvic dataset and in second case, from 3T MRI data, 7T MRI data is estimated. Separately, results of experimentation for two different tasks are described.

3.1 PSNR performance comparison

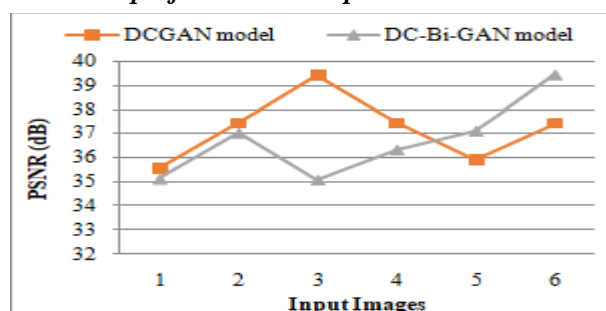


Fig.3. PSNR performance comparison

Fig.3 shows that the PSNR comparison results between Existing DCGAN Based Method and Proposed DC-Bi-GAN based Method. The proposed method has high value of PSNR. From results, it is well know that proposed method obtain high PSNR indicating the good lung nodule detection. Because, the proposed scheme is based on excellent feature extraction and DC-Bi-GAN based concept is enhancing the learning efficiency. When comparing the PSNR rate among the existing methods at the same image size are providing fewer rates which indicates the proposed work can give better synthesis results than the existing method.

3.2 MSE performance comparison

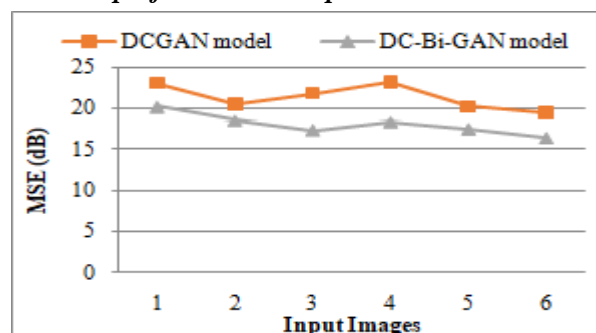


Fig.4. MSE performance comparison

Fig.4 shows that the MSE comparison results between Existing DCGAN Based Method and Proposed DC-Bi-

GAN based Method. The proposed method has low value of MSE. From results, it is well know that proposed method obtain less error value indicating the good detection rate. Because, the proposed scheme is having the effective image enhancement stage which reduce the noises. When comparing the PSNR rate among the existing methods at the same image size, providing high error rate which shows the proposed work can give better detection results than the existing method.

3.3 SSIM performance comparison

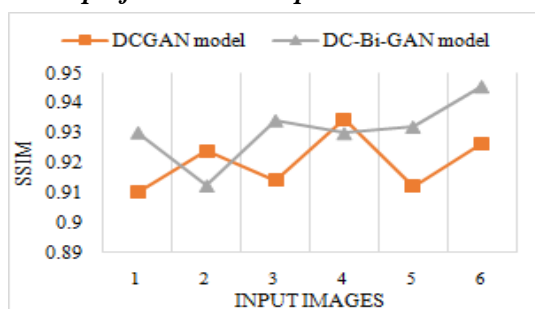


Fig.5. SSIM performance comparison

Fig.5 shows that the SSIM comparison results between exiting DCGAN based method and proposed DC-Bi-GAN based Method. From figure, proposed method can obtain high SSIM when compared to existing methods. It is an effective way of getting the lung nodule accurately with the high SSIM rate of 0.9456 at the image size is 6. When comparing the SSIM among the existing methods at the same image size of 6, providing less rate. Through the results, it can be seen that the proposed work is much better than the existing method.

3.4 Execution Time performance comparison

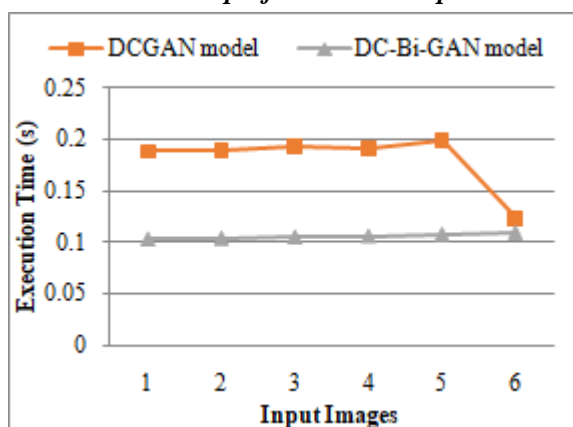


Fig.6. Execution Time performance comparison

Fig.6 shows that the execution time comparison results between exiting DCGAN based method and proposed DC-Bi-GAN based Method. From figure, proposed method can have less execution time when compared to existing methods. It is an effective way of getting the lung nodule accurately with the less execution time of

0.1096s at the image size is 6. When comparing the execution time results among the existing, all are providing high rate. Through the results, it can be seen that the proposed work is much better than the existing method.

3.5 Detection Accuracy

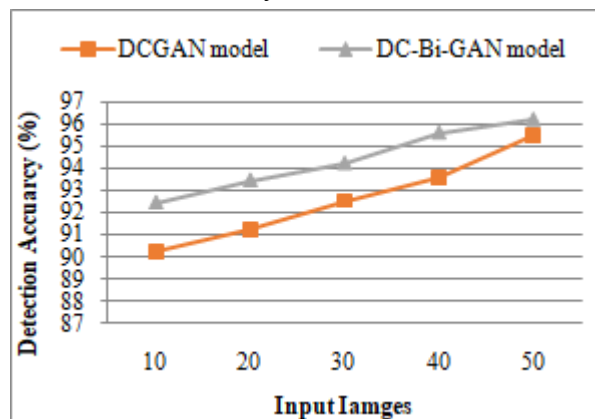


Fig.7. Detection Accuracy Vs No. of Images

Fig.7 shows combined detection accuracy of Existing DCGAN based method and proposed DC-Bi-GAN based method under number of images. It is observed that the detection accuracy of proposed method is greater than existing scheme. From figure, it is observed that when the number of images increases, the average DA reduces in existing method. When proposed method is implemented, the average detection accuracy of proposed method and existing method are 96.25%, and 95.47% respectively. The reason is that; the genetic algorithm with DC-Bi-GAN will improve the rib suppression and nodule detection with an effective manner using deep convolutional network.

4 Conclusion and future work

From source images, target images are estimated by proposing supervised deep convolutional model through adversarial learning in this research. With genetic algorithm, images are estimated from various modality classes. Generated target image is enhanced by introducing special loss function. Long term residual connection is established by extending residual learning unit. This is used to train the network in an easy manner. ACM is used to enhance the performance iteratively. During training process, effectively enlarge the Bi-GAN context. This makes the awareness about context. On two tasks, proposed model is validated. From MRI data CT data is predicted and 7T MRI is formed from 3T MRI. In all dataset and task, proposed model shows superior performance than the existing models. Different medical images can be synthesized by using proposed method as indicated by results of experimentation.

References

1. Y. Berker, J. Franke, A. Salomon, M. Palmowski, H. C. Donker, Y. Temur, F. M. Mottaghy, C. Kuhl, D. Izquierdo-Garcia, Z. A. Fayad et al., "Mri-based attenuation correction for hybrid pet/mri systems: a 4-class tissue segmentation technique using a combined ultrashort-echo-time/dixonmri sequence," *Journal of nuclear medicine*, vol. 53, no. 5, pp. 796–804, 2012.
2. C. Catana, A. van der Kouwe, T. Benner, C. J. Michel, M. Hamm, M. Fenchel, B. Fischl, B. Rosen, M. Schmand, and A. G. Sorensen, "Toward implementing an mri-based pet attenuation-correction method for neurologic studies on the mr-pet brain prototype," *Journal of Nuclear Medicine*, vol. 51, no. 9, pp. 1431–1438, 2010.
3. D. H. Ye, D. Zikic, B. Glocker, A. Criminisi, and E. Konukoglu, *Modality Propagation: Coherent Synthesis of Subject-Specific Scans with Data-Driven Regularization*. Berlin, Heidelberg: Springer Berlin Heidelberg, 2013, pp. 606–613
4. N. Burgos, M. J. Cardoso, K. Thielemans, M. Modat, S. Pedemonte, J. Dickson, A. Barnes, R. Ahmed, C. J. Mahoney, J. M. Schott, J. S. Duncan, D. Atkinson, S. R. Arridge, B. F. Hutton, and S. Ourselin, "Attenuation correction synthesis for hybrid pet-mr scanners: Application to brain studies," *IEEE Transactions on Medical Imaging*, vol. 33, no. 12, pp. 2332–2341, Dec 2014.
5. J. V. Manjon, P. Coup ´ e, A. Buades, D. L. Collins, and M. Robles, "Mrisuperresolution using self-similarity and image priors," *Journal of Biomedical Imaging*, vol. 2010, p. 17, 2010.
6. A. Jog, A. Carass, and J. L. Prince, "Improving magnetic resonance resolution with supervised learning," in *Biomedical Imaging (ISBI), 2014 IEEE 11th International Symposium on*. IEEE, 2014, pp. 987–990.
7. T. Huynh, Y. Gao, J. Kang, L. Wang, P. Zhang, J. Lian, and D. Shen, "Estimating ct image from mri data using structured random forest and auto-context model," *IEEE transactions on medical imaging*, vol. 35, no. 1, pp. 174–183, 2016.
8. Zhao C., Carass A., Lee J., He Y., Prince J.L. Whole brain segmentation and labeling from CT using synthetic MR images; *Proceedings of the International Workshop on Machine Learning in Medical Imaging; Quebec City, QC, Canada. 10 September 2017; pp. 291–298.*
9. Ronneberger O., Fischer P., Brox T. U-Net: Conconvlutional Networks for Biomedical Image Segmentation; *Proceedings of the International Conference on Medical Image Computing and Computer-Assisted Intervention; Munich, Germany. 5–9 October 2015; pp. 234–241.*
10. Nie D., Trullo R., Lian J., Petitjean C., Ruan S., Wang Q., Shen D. Medical image synthesis with context-aware generative adversarial networks; *Proceedings of the International Conference on Medical Image Computing and Computer-Assisted Intervention; Quebec City, QC, Canada. 11–13 September 2017; pp. 417–425.*
11. Bi L., Kim J., Kumar A., Feng D., Fulham M. Molecular Imaging, Reconstruction and Analysis of Moving Body Organs, and Stroke Imaging and Treatment. Springer International Publishing AG; Cham, Switzerland: 2017. Synthesis of positron emission tomography (pet) images via multi-channel generative adversarial networks (gans) pp. 43–51.
12. Isola P., Zhu J.-Y., Zhou T., Efros A.-A. Image-to-image translation with conditional adversarial networks; *Proceedings of the IEEE Conference on Computer Vision and Pattern Recognition (CVPR); Honolulu, HI, USA. 21–26 July 2017; pp. 1–10.*
13. Ben-Cohen A., Klang E., Raskin S.-P., Amitai M.-M., Greenspan H. Virtual pet images from ct data using deep convolutional networks: Initial results; *Proceedings of the International Workshop on Simulation and Synthesis in Medical Imaging; Quebec City, QC, Canada. 10 September 2017; pp. 49–57.*
14. Long J., Shelhamer E., Darrell T. Fully convolutional networks for semantic segmentation; *Proceedings of the IEEE Conference on Computer Vision and Pattern Recognition (CVPR); Boston, MA, USA. 7–12 June 2015; pp. 3431–3440.*
15. R. Vemulapalli, H. V. Nguyen, and S. K. Zhou, "Unsupervised crossmodal synthesis of subject-specific scans," in *2015 IEEE International Conference on Computer Vision (ICCV), Dec 2015, pp. 630–638.*
16. A. Krizhevsky, I. Sutskever, and G. E. Hinton, "Imagenet classification with deep convolutional neural networks," in *Advances in neural information processing systems*, 2012, pp. 1097–1105.
17. C. Dong, C. C. Loy, K. He, and X. Tang, "Learning a deep convolutional network for image super-resolution," in *European Conference on Computer Vision*. Springer, 2014, pp. 184–199.
18. J. Kim, J. Kwon Lee, and K. Mu Lee, "Deeply-recursive convolutional network for image super-resolution," in *Proceedings of the IEEE Conference on Computer Vision and Pattern Recognition*, 2016, pp. 1637–1645.
19. R. Li, W. Zhang, H.-I. Suk, L. Wang, J. Li, D. Shen, and S. Ji, "Deep learning based imaging data completion for improved brain disease diagnosis," in

- International Conference on Medical Image Computing and Computer-Assisted Intervention. Springer, 2014, pp. 305–312.
20. Y. Huang, L. Shao, and A. F. Frangi, “Simultaneous super-resolution and cross-modality synthesis of 3d medical images using weakly-supervised joint convolutional sparse coding,” arXiv preprint arXiv:1705.02596, 2017.
 21. C. Dong, C. C. Loy, K. He, and X. Tang, “Image super-resolution using deep convolutional networks,” IEEE transactions on pattern analysis and machine intelligence, vol. 38, no. 2, pp. 295–307, 2016.
 22. M. Mathieu, C. Couprie, and Y. LeCun, “Deep multi-scale video prediction beyond mean square error,” arXiv preprint arXiv:1511.05440, 2015.
 23. C. Ledig, L. Theis, F. Huszar, J. Caballero, A. Cunningham, A. Acosta, A. Aitken, A. Tejani, J. Totz, Z. Wang et al., “Photo-realistic single image super-resolution using a generative adversarial network,” arXiv preprint arXiv:1609.04802, 2016.